

## Part II: Lithium disilicate ( $\text{Li}_2\text{Si}_2\text{O}_5$ ): Mild Condition Hydrothermal synthesis, Characterization and Optical Properties

Abdolali Alemi<sup>a</sup>, Shahin Khademinia<sup>a\*</sup> Murat Sertkol<sup>b</sup>

<sup>a</sup> Department of Inorganic Chemistry, Faculty of Chemistry, University of Tabriz, Tabriz, Iran

<sup>b</sup> Department of Physics Engineering, Istanbul Technical University, Maslak, 34469, TR.

### Article history:

Received 3/10/2014

Accepted 9/11/2014

Published online 21/12/2014

### Keywords:

Lithium Disilicate

Hydrothermal Method

Nano Materials

PXRD

FESEM

### \*Corresponding author:

Shahin khademinia

E-mail address:

shahinkhademinia@gmail.com

Phone: 98 9116224110

### Abstract

Lithium disilicate nano-powders were synthesized via a mild condition hydrothermal reaction at 180 °C for 48 and 72 h with a non stoichiometric 1:2 Li:Si molar ratio in NaOH aqueous solution using  $\text{Li}_2\text{CO}_3$  and  $\text{SiO}_2 \cdot \text{H}_2\text{O}$  as raw materials. The synthesized materials were characterized by powder X-ray diffraction (PXRD) technique and Fourier transform infrared (FTIR) spectroscopy. The XRD data showed that the obtained materials crystallized in a monoclinic crystal structure with a space group of Ccc2. The morphologies of the synthesized nanomaterials were studied by field emission scanning electron microscope (FESEM). Ultraviolet–visible spectra showed that the nanostructured lithium disilicate powders had good light absorption properties in the ultraviolet light region. Photo luminescence spectra of the obtained materials were investigated in an excitation wavelength of 281 nm. Cell parameter refinement data of the obtained materials showed that with increasing the reaction time, parameters a and b were increased. So there is an expansion in the unit cell.

2014 JNS All rights reserved

## 1. Introduction

Lithium ceramics have some technological applications. Among these ceramics, lithium silicates have been investigated as breeder materials for nuclear fusion reactors, carbon dioxide absorbents, thermal expansion of glass ceramics and so many other applications [1-7]. Lithium disilicate is used as pyroelectric materials

in optical waveguide devices [8-13]. Different experimental syntheses have been reported to synthesize  $\text{Li}_2\text{Si}_2\text{O}_5$  nano materials such solid state reaction, precipitation, sol–gel method, extrusion-spherodisation process, rotating/melting procedures, combustion, electrochemical method, and recently via hydrothermal method. However, most of the time, a mixture of  $\text{Li}_2\text{SiO}_3$ ,  $\text{Li}_2\text{Si}_2\text{O}_5$ ,  $\text{Li}_4\text{SiO}_4$ , and  $\text{SiO}_2$  were obtained [14, 15, 18-23].

Recently, we have reported the synthesis of highly crystalline and pure lithium disilicate nanomaterials through a mild condition via hydrothermal method at 180°C with lithium nitrate and silicic acid as raw materials at 1:3 Li:Si molar ratio [24]. In the present study, a hydrothermal route was explored successfully to synthesize nanostructure  $\text{Li}_2\text{Si}_2\text{O}_5$  powders in a hydrothermal system of  $\text{Li}_2\text{CO}_3$ ,  $\text{SiO}_2\cdot\text{H}_2\text{O}$  and NaOH. To the best of our knowledge, there is no report on the synthesis of nanostructure  $\text{Li}_2\text{Si}_2\text{O}_5$  crystallites by these raw materials.

## 2. Materials and methods

All chemicals were of analytical grade, obtained from commercial sources, Merck Company, and used without further purification. Phase identifications were performed on a powder X-ray diffractometer D5000 (Siemens AG, Munich, Germany) using  $\text{CuK}\alpha$  radiation. The morphology of the obtained materials was examined with a field emission scanning electron microscope (Hitachi FE-SEM model S-4160). Also, FT-IR spectra were recorded on a Tensor 27 (Bruker Corporation, Germany). Absorption and photoluminescence spectra were recorded on a Jena Analytik Specord 40 (AnalytikJena UK, Wembley, UK) and a PerkinElmer LF-5 spectrometer (PerkinElmer, Waltham, MA, USA), respectively. Also, cell parameter refinement was reported by celref software version 3.

### 2.1. Experimental

In a typical synthetic experiment, 0.300 g (4.0 mmol) of  $\text{Li}_2\text{CO}_3$  ( $M_w = 73.82 \text{ g mol}^{-1}$ ) and 0.96 g (16.0 mmol) of  $\text{SiO}_2\cdot\text{H}_2\text{O}$  ( $M_w = 60.08 \text{ g mol}^{-1}$ ) were added to 60 mL of hot aqueous solutions of 0.4M NaOH under magnetic stirring at 80°C. The resultant solution was stirred further for 15 min.

The obtained solution was transferred into a 100-mL Teflon lined stainless steel autoclave. The autoclave was sealed and heated at 180°C for 48 (sample 1) or 72 h (sample 2). When the reaction was completed, it cooled to room temperature by water immediately. The prepared powder washed with distilled water and dried at 110°C for 20 min under normal atmospheric conditions. And allowed to cool slowly to room temperature, a white powder was collected.

## 3. Result and discussion

### 3.1. Powder X-ray diffraction analysis

The crystal phases of the synthesized nanomaterials with different reaction times for 48 ( $S_1$ ) and 72( $S_2$ ) h at 180°C were examined by powder X-ray diffraction technique. As shown in figure 1, a pure highly crystalline phase of meta-stable  $\text{Li}_2\text{Si}_2\text{O}_5$  with Primitive orthorhombic Bravais Lattice (space group of Pbcn) [14, 24-26] was obtained after 48 h. By increasing the reaction time to 72h, a mixture of meta-stable  $\text{Li}_2\text{Si}_2\text{O}_5$  (space group of Pbcn) and  $\text{Li}_2\text{SiO}_3$  with base-centered orthorhombic Bravais Lattice (space group of Cmc2<sub>1</sub>) was obtained. The additional peaks in figure 1a at 2 theta in about 18.9, 26.9 and 33.2 degrees are related to  $\text{Li}_2\text{SiO}_3$  impurity phase, and the peaks at about 11, 28 and 35 are corresponded to the residual  $\text{SiO}_2$  and  $\text{Li}_2\text{O}$  (created from lithium carbonate in aqueous solution) [18-23]. However, as reported in some papers, a stable form of lithium disilicate crystallizes with base-centered monoclinic Bravais Lattice (the space group of Ccc2) [27]. According to the XRD patterns, they show that with using lithium carbonate in replacement of lithium nitrate as lithium ion source, the main phase is lithium disilicate in replacement of lithium metasilicate. However, there is a mixture of lithium metasilicate and lithium disilicate phases

at 72h; while at 48h, there is a pure lithium disilicate phase. But, in our another published work, using 1:2 Li:Si molar ratio, the main phase was lithium metasilicate and with 1:3 Li:Si molar ratio the main phase was lithium disilicate. So, we can conclude that the metal salt is a main factor to synthesize a specific phase [7]. Interplanar spacing ( $d$ ) in the obtained crystalline material is calculated via Bragg's equation ( $n\lambda = 2d_{hkl} \sin\theta$ ). Thus compared to those of the obtained materials at 48 h, with increasing the reaction time, the diffraction lines in the powder XRD patterns of the nanoparticles of lithium disilicate shift to a lower  $2\theta$  values ( $\Delta 2\theta = 24.67(48 \text{ h}) - 24.60(72 \text{ h}) = 0.07^\circ$  and  $\Delta d = 3.614 \text{ \AA} (72 \text{ h}) - 3.277 \text{ \AA} (48 \text{ h}) = 0.337 \text{ \AA}$ ). So, according to above calculations, there is an expansion in the unit cell with increasing the reaction time from 48 to 72h.

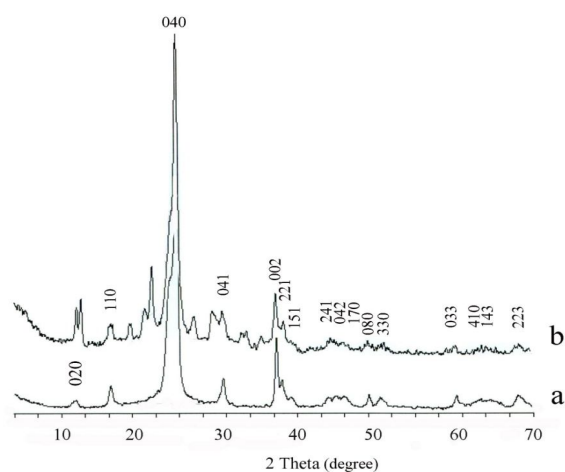


**Fig. 1.** PXRD patterns of the synthesized  $\text{Li}_2\text{Si}_2\text{O}_5$  nanoparticles, where a is  $S_1$ ; b is  $S_2$  at  $180^\circ\text{C}$ .

Table 1 shows the crystal sizes of the as-synthesized nanomaterials in different NaOH molar ratios calculated via Scherrer equation, using the peak at  $h k l$  (040) corresponds to  $\text{Li}_2\text{Si}_2\text{O}_5$  phase,

$$t = \frac{k\lambda}{B_{1/2} \cos\theta}$$

where  $t$  is entire thickness of the

crystalline sample,  $\lambda$  is the x-ray diffraction wavelength and is 0.154 nm,  $k$  is the Scherrer constant and is 0.9,  $B_{1/2}$  of FWHM is the full width at half its maximum intensity and  $\Theta_B$  is the half diffraction angle at which the peak location is.

**Table 1.** Calculated Scherrer data for pure  $\text{Li}_2\text{Si}_2\text{O}_5$  nanomaterials  $S_1$  and  $S_2$  at  $180^\circ\text{C}$  in 0.4M NaOH solution.

Sample	$2\theta$	$\theta$ value	$B_{1/2}$ (degree)	$B_{1/2}$ (radian)	$\cos\theta_B$	$t(\text{nm})$
$S_1$	24.67	12.335	0.657	0.0114	0.9769	12.37
$S_2$	24.60	12.300	0.427	0.0074	0.9770	19.04

### 3.2. Morphology analysis

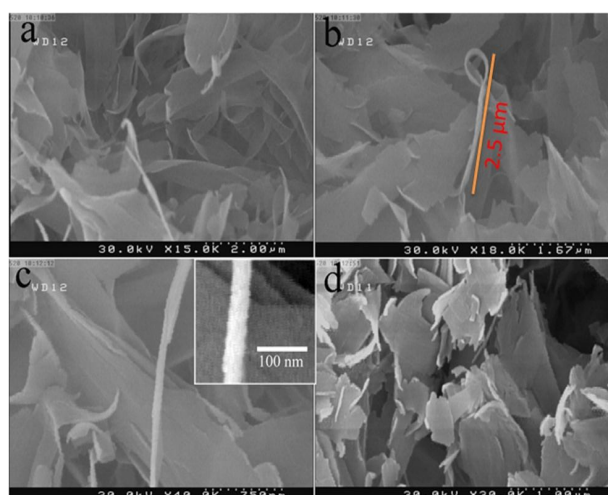


**Fig. 2.** SEM images of  $S_1$ .

Figure 2 represents the SEM images of  $S_2$  at  $180^\circ\text{C}$ . Figure 2 shows that after 48h, the morphology of the obtained material is layer-like, consisting of sheets with no regular edge shape. Figure 2 (a and b) and d show the layer structure of the as-prepared materials with no significant orientation. Figure 2c shows a high magnification image of the obtained material. It shows that the width size of the materials is about 50-60 nm with the length size of (figure 2b) about 2.5  $\mu\text{m}$ .

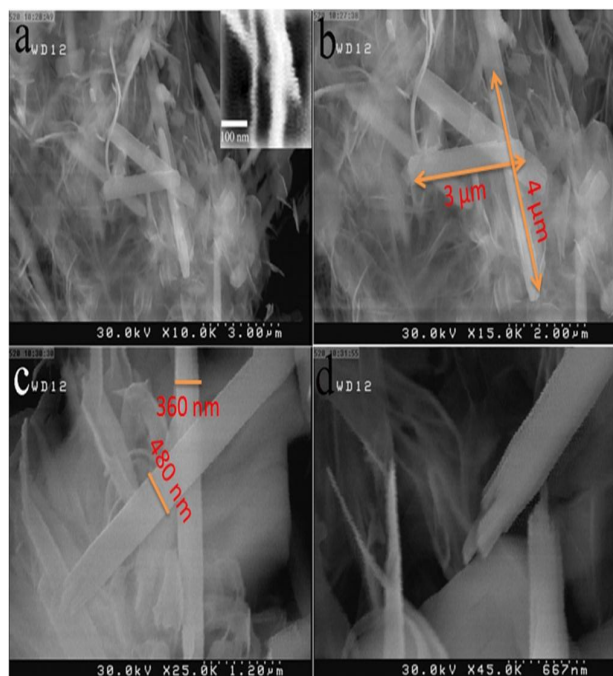


**Fig. 3.** SEM images of ( $S_2$ ).

Figure 3 shows typical FESEM images of the  $S_2$  at  $180^\circ\text{C}$ . From the typical FESEM images of  $S_2$ , at low magnification in figure 3 (a and b) we can see that with increasing the reaction time from 48h to 72h, the morphology of the obtained materials are in a nearly rod and wire forms and the rods have nearly homogenous morphology with the size of about 3-4  $\mu\text{m}$  in length, and 360-480 nm in width and the wires with the size of about 60 nm in thickness and 2-3 $\mu\text{m}$  in length, as shown in figure 3b and c. However, as shown in figure 3c, the whole sizes of the obtained materials (layers compared to rod structure) synthesized at 72h are larger than that of 48h. Also, with comparing to our another work [7], with using lithium carbonate as lithium ion source at 1:2 Li:Si molar ratio, in replacement of lithium nitrate, at 1:2 molar ratio, the morphology of the obtained materials in the case of lithium disilicate changed to nano rods and layers. So, it shows that the reactant type is a main factor affect on the morphology of the obtained materials [7].

Table 2 shows the cell parameter refinement data of the synthesized nanomaterials. It is clear that parameters a and b values of the as-synthesized materials are larger and parameter c is smaller than those of the standard sample. However, parameters a and b for  $S_2$  are larger than those of  $S_1$  but parameter c for  $S_2$  is smaller than that of  $S_1$ . Because, in SEM images we found that the particle sizes of the  $S_2$  are larger than those of  $S_1$ , so we can conclude that parameter a and b are the main factor on the size of the materials [24].

**Table 2.** Cell parameter refinement plot of  $\text{Li}_2\text{Si}_2\text{O}_5$  showing an expansion along the a and b directions in the unit cell.

Sample	a	b	c
JCPDS:14-322)	5.80	14.66	4.81
Sample 1	5.84	14.49	4.80
Sample 2	5.85	14.51	4.80

### 3.3. Optical properties

Figure 4 shows the FTIR spectra of the synthesized materials  $S_1$  and  $S_2$  at  $180^\circ\text{C}$ . It is clear that the peaks at 467.27 and 557.21  $\text{cm}^{-1}$  are assigned to O-Si-O bending vibration and the peaks at 650.61, 759.41 and 766.27  $\text{cm}^{-1}$  are assigned to symmetric stretching vibration of Si-O-Si. Also, the peaks at 932.94, 111.26 and 1253.86  $\text{cm}^{-1}$  are assigned to asymmetric stretching vibration of Si-O-Si and the peak at 3422.80  $\text{cm}^{-1}$  is assigned to the vibration for  $\text{H}_2\text{O}$  [28, 29].

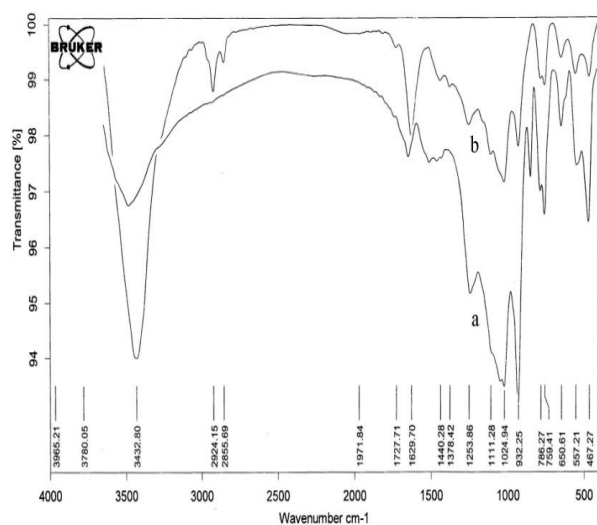
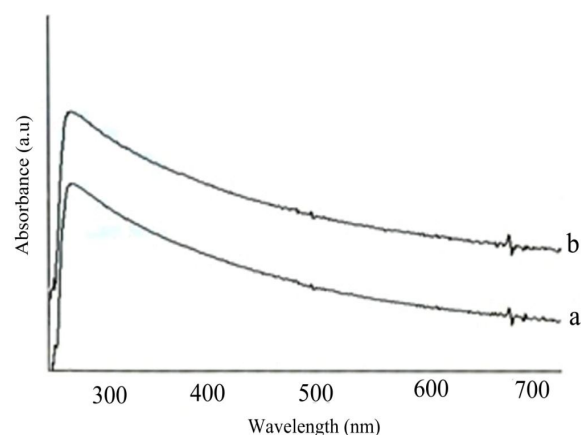


**Fig. 4.** FTIR spectra of the synthesized  $\text{Li}_2\text{Si}_2\text{O}_5$  nanomaterials, where a is  $\text{S}_1$  and b is  $\text{S}_2$ .

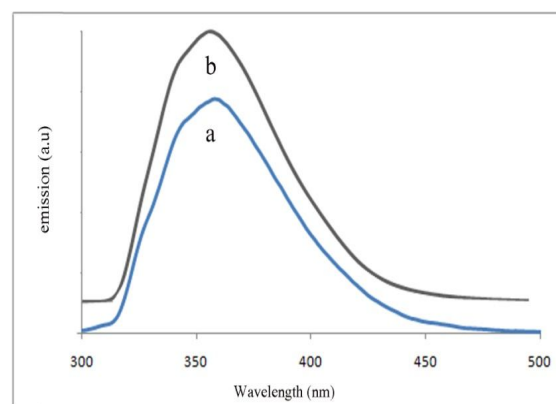
Figure 5 shows UV–visible spectra of the pure phase  $\text{Li}_2\text{Si}_2\text{O}_5$  powders produced by the hydrothermal reaction at  $180^\circ\text{C}$  for 48 and 72h, respectively. No obvious difference could be detected from two UV–visible spectra, except for a slight little blue shift of nano materials synthesized at 72h relative to that of 48h. A sharp absorption band at 283 and 278 nm is observed respectively for  $\text{S}_1$  and  $\text{S}_2$ . The band gap energy estimated from UV–visible is 4.38 eV, and 4.46 eV. According to our another works on the synthesis of lithium silicates, we found that with increasing the reaction time from 48 to 72h, and increasing the particle size, there is a blue shift in the absorption wavelength and so the calculated band gap is increased [30]. So we can conclude that the particle size is a factor on the calculated band gap. It means that for increasing the band gap we should increase the particle size.

Figure 6 represents the room-temperature emission spectra of the as-synthesized materials under excitation at 281 nm. A strong broad emission band at 357 and 358 nm is observed for  $\text{S}_1$

and  $\text{S}_2$ , respectively. So, there is a red shift in the emission spectra with increasing the reaction time from 48 to 72h.



**Fig. 5.** UV-vis spectra of the synthesized  $\text{Li}_2\text{Si}_2\text{O}_5$  nanomaterials, where a is  $\text{S}_1$  and b is  $\text{S}_2$ .



**Fig. 6.** Photoluminescence spectra of the synthesized  $\text{Li}_2\text{Si}_2\text{O}_5$  nanomaterials ( $\lambda_{\text{ex}} = 281 \text{ nm}$ ), where a is  $\text{S}_1$  and b is  $\text{S}_2$ .

#### 4. Conclusion

In summary, uniform rod and layer like lithium disilicate were successfully synthesized by a simple hydrothermal method. We found that the reaction time has a main effect on the morphology of the products. UV–vis electronic absorption and emission spectra of the synthesized materials were investigated. Also, cell parameter refinement was

calculated by celref software version 3 and showed that the parameters have influences on the size of the obtained materials.

### Acknowledgements

The authors express their sincere thanks to the authorities of Tabriz University for financing the project.

### References

- [1] H. Kudo, K. Okuno, S. Ohira, *J. Nucl. Mater.* 155 (1988) 524.
- [2] G. Wen, X. Zheng, L. Song, *Acta. Mater.* 55 (2007) 3583.
- [3] T Yamaguchi, B.N. Nair, K. Nakagawa, *J. Membr. Sci.* 294 (2007) 16.
- [4] K. Essaki, M. Kato, K. Nakagawa, *J. Ceram. Soc. Japan.* 114 (2006) 739.
- [5] H. Pfeiffer, P. Bosch, S. Bulbulian, *J. Nucl. Mater.* 257 (1998) 309.
- [6] H.A. Mosqueda, C. Vazquez, P. Bosch, H. Pfeiffer, *Chem. Mater.* 18 (2006) 2307.
- [7] A. Alemi, S. Khademinia, S. Woo Joo, M. Dolatyari, A. Bakhtiari, *Inter. Nano Let.* 3 (2013) 14.
- [8] G.D. Ilyushin, *J. Inorg. Mater.* 9 (2002) 927.
- [9] G.B. Kumar, S. Buddhudu, *Ceram. Int.* 35 (2009) 521.
- [10] W.R. Romanowski, I. Sokolska, G.D. Dsik, S. Golab, *J. Alloys Compd.* 300-301 (2000) 152.
- [11] D. Hreniak, A. Speghini, M. Bettinelli, W. Streck, *J. Lumin.* 119–120 (2006) 219.
- [12] X. Yang, G. Ning, X. Li, Y. Lin, *Mater. Lett.* 61 (2007) 4694.
- [13] M. Ignatovych, V. Holovey, T. Vidczy, P. Baranyai, *Radiat. Phys. Chem.* 76 (2007) 1527.
- [14] M.P. Vinod, D. Bahnemann, *J. Solid State Electrochem.* 7 (2002) 498.
- [15] D. Cruz, S. Bulbulian, E. Lima, H. Pfeiffer, *J. Solid State Chem.* 179 (2006) 909.
- [16] M. Taddia, P. Modesti, A. Albertazzi, *J. Nucl. Mat.* 336 (2005) 173.
- [17] H. Pfeiffer, P. Bosch, S. Bulbulian, *J. Nucl. Mat.* 257 (1998) 309.
- [18] J.G. van der Laan, H. Kawamura, N. Roux, D. Yamaki, *J. Nucl. Mat.* 283 (2000) 99.
- [19] D. Cruz, S. Bulbulian, *J. Am. Ceram. Soc.* 88 (2005) 1720.
- [20] J. Ortiz-Landeros, M.E. Contreras-García, C. Gómez-Yáñez, H. Pfeiffer, *J. Solid State Chem.* 184 (2011) 1304-1311.
- [21] T. Tang, Z. Zhang, J.B. Meng, D.L. Luo, *Fusion Engineering and Design.* 84 (2009) 2124-2130.
- [22] A. Alemi, S. Khademinia, M. Dolatyari, A. Bakhtiari, *Int. Nano Lett.* 2 (2012) 20.
- [23] R.I. Smith, R.A. Howie, A.R. West, A.A. Pina, M.E. Villafuerte-Castrejón, *Acta Crystal. Sect. C.* 46 (1990) 363.
- [24] R.I. Smith, A.R. West, I. Abrahams, P.G. Bruce, *Powder Diffraction.* 5 (1990) 137.
- [25] B.H.W.S. Dejong, H.T.J. Supér, A.L. Spek, N. Veldman, G. Nachtegaal, J.C. Fischer, *Acta Crystal. Sect. B.* 54 (1998) 568.
- [26] G. D. Ilyushin, *Inorganic Materials.* 38 (2002) 927–933.
- [27] M. Mohamed Mahmoud, Blacksburg, Virginia. 24 (2007).
- [28] A. Alemi, S. Woo Joo, S. Khademinia, M. Dolatyari, A. Bakhtiari, H. Moradi, S. Saeidi, *Inter. Nano Let.* 3 (2013) 38-43.